

# Gas-phase Protonation of Pyridine. A Variable-time Neutralization–Reionization and *Ab Initio* Study of Pyridinium Radicals

Viet Q. Nguyen and František Tureček\*

Department of Chemistry, Bagley Hall, Box 351700, University of Washington, Seattle, Washington 98195-1700, USA

Gas-phase protonation of pyridine with  $\text{CH}_3\text{NH}_3^+$ ,  $\text{NH}_4^+$ ,  $t\text{-C}_4\text{H}_9^+$ ,  $\text{H}_3\text{O}^+$  and  $\text{CH}_5^+$  under thermal conditions was studied by variable-time neutralization–reionization mass spectrometry and *ab initio* calculations. N-Protonation was found to occur exclusively for  $\text{CH}_3\text{NH}_3^+$  through  $\text{H}_3\text{O}^+$  and predominantly for  $\text{CH}_5^+$ . The calculated MP2/6–311G(2d,p) energies gave the proton affinities of N, C-2, C-3 and C-4 in pyridine as 924, 658, 686 and 637  $\text{kJ mol}^{-1}$ , respectively, which were in good agreement with previous experimental and theoretical results. Vertical neutralization of the N-protonated isomer ( $1\text{H}^+$ ) was accompanied by moderate Franck–Condon effects that deposited 20–21  $\text{kJ mol}^{-1}$  in the  $1\text{H}$ -pyridinium radicals ( $1\text{H}^\cdot$ ) formed.  $1\text{H}^\cdot$  was calculated by UMP2/6–311G(2d,p) and B3LYP/6–311G(2d,p) to be a bound species in its ground electronic state. A substantial fraction of stable  $1\text{H}^\cdot$  was detected in the spectra, which depended on the precursor ion internal energy. Deuterium labeling showed a specific loss of the N-bound hydrogen or deuterium in the radicals. The specificity increased with increasing internal energy in the radicals and decreasing contribution of ion dissociations following reionization. Variable-time measurements established specific loss of the N-bound deuterium also in dissociating low-energy  $1\text{D}^\cdot$ . Loss of hydrogen from  $1\text{H}^+$  cations following reionization was highly endothermic and was accompanied by rearrangements that partially scrambled the ring hydrogens.

*J. Mass Spectrom.* 32, 55–63 (1997)

No. of Figures: 9 No. of Tables: 2 No. of Refs: 36

KEYWORDS: pyridine; proton affinity; variable-time neutralization–reionization; *ab initio* calculations, deuterium labeling

## INTRODUCTION

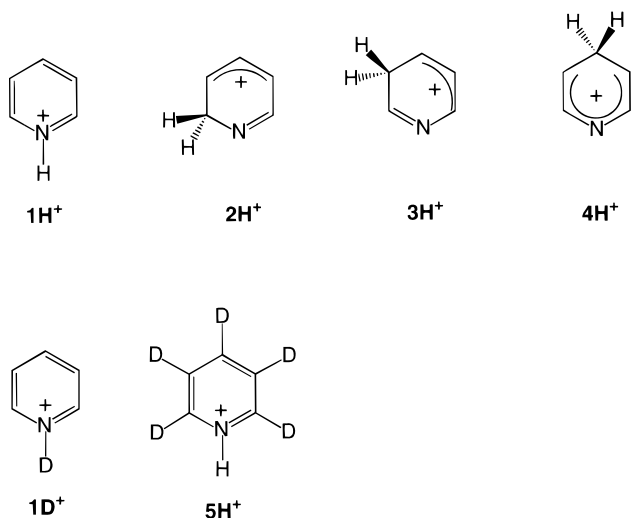
Pyridine (**1**) and its substituted derivatives have been used as reference bases in numerous gas-phase basicity measurements and their proton affinities are well known.<sup>1,2</sup> Protonation of gaseous pyridine presumably takes place at the nitrogen atom rather than in one of the ring positions, by analogy with the formation of pyridinium salts in solution.<sup>3</sup> Experimental proton affinities of the C-2, C-3 and C-4 ring carbons in pyridine are unknown. However, recent *ab initio* calculations showed convincingly that the nitrogen atom is by far the most basic site in gaseous pyridine, followed by C-3, C-2 and C-4 in order of decreasing proton affinities.<sup>4</sup> Equilibrium gas-phase basicity measurements probe the most basic site in the molecule, e.g. the nitrogen atom in pyridine. In contrast, chemical ionization with gas-phase acids much stronger than pyridinium ( $1\text{H}^+$ ) can result in proton transfer to the less basic C-2 through C-4 positions to form the less stable tautomers  $2\text{H}^+$  through  $4\text{H}^+$ . For example, protonation of these positions with  $\text{CH}_5^+$  of proton affinity  $\text{PA}(\text{CH}_4) =$

545–552  $\text{kJ mol}^{-1}$  (Refs 2 and 5) is estimated to be  $>90$   $\text{kJ mol}^{-1}$  exothermic<sup>4</sup> and could occur under chemical ionization conditions.

We have shown recently, having followed a previous study by Harrison and co-workers,<sup>6</sup> that protonation sites in gaseous heterocycles can be determined by combining neutralization–reionization mass spectrometry (NRMS)<sup>7</sup> with deuterium labeling.<sup>8</sup> Our approach was to distinguish by labeling the hydrogen atoms present in the gaseous molecule from the proton introduced by the gas-phase acid and to use unimolecular dissociations of radical intermediates, generated by vertical reduction, to determine the site of proton or deuterium attachment in the ion (Scheme 1). For pyridine in particular, gas-phase deuteration at the nitrogen atom creates a stable aromatic cation  $1\text{D}^+$ . Vertical neutralization converts  $1\text{D}^+$  to the anti-aromatic radical  $1\text{D}^\cdot$ , which has the same bond connectivity and initial geometry as the precursor cation. Assuming that  $1\text{D}^\cdot$  dissociates by simple N–D bond cleavage to recreate pyridine, the latter should not contain the label introduced by deuteration. In case of C-deuteration, the intermediate radical (e.g.  $2\text{D}^\cdot$ ) can lose either H or D from the methylene group to regenerate labeled or unlabeled neutral pyridine. A complementary experiment involving protonation of a labeled pyridine is necessary to assess the kinetic isotope effects on the loss H and D from the ring positions.<sup>8</sup>

\* Correspondence to: F. Tureček.

Contract grant sponsor: National Science Foundation;  
Contract grant number: CHE-9412774.



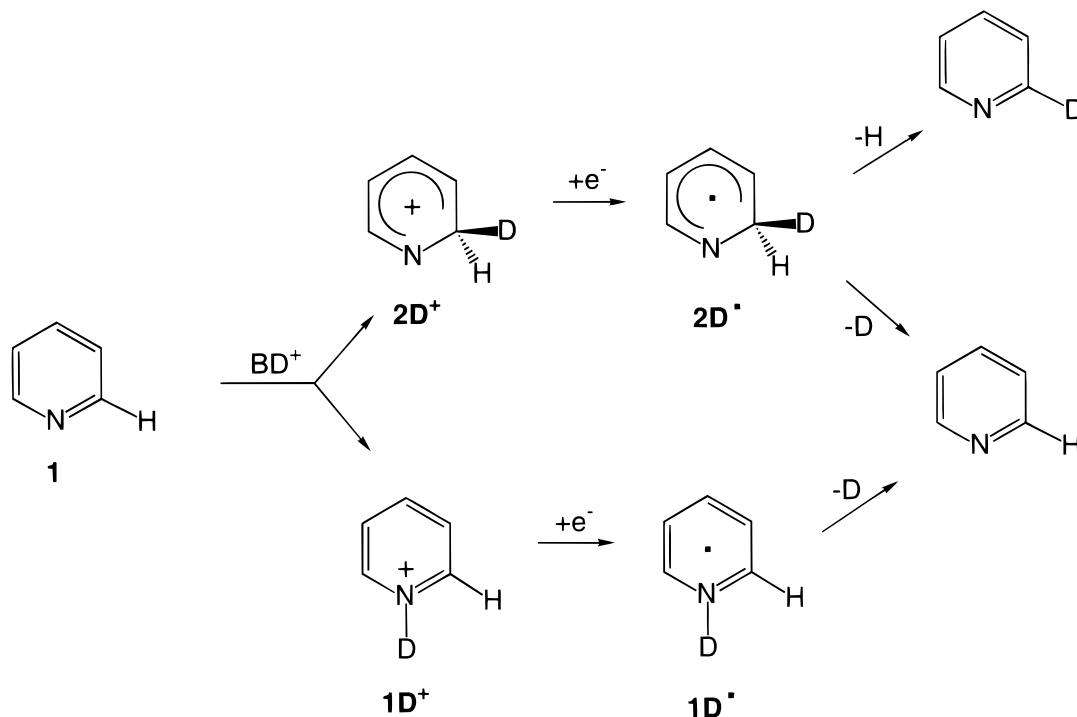
The foregoing simple scheme was shown to work reasonably well for protonation of pyrrole and imidazole.<sup>8</sup> Other systems, e.g. aniline<sup>9</sup> and glycine,<sup>10</sup> were also shown to be amenable to neutralization–reionization studies. However, with less favorable systems complications may occur owing to (i) unimolecular tautomerization in the precursor cations, (ii) isomerization in the intermediate radicals, (iii) isomerization in the reionized cations and (iv) C–H bond dissociations that produce isomeric structures, e.g. pyridine ylides.<sup>11</sup>

In this work, we used the recently introduced variable-time NRMS<sup>12,13</sup> to distinguish isomerizations and dissociations of intermediate pyridinium radicals from those of cations induced by collisional reionization. In this method, the observation times for neutral and ion dissociations are varied simultaneously, but in an opposite sense.<sup>13</sup> This allows not only detection of short-lived species of sub-microsecond lifetimes,<sup>14</sup> but also determination of unimolecular rate parameters in

neutral intermediates and ions following reionization.<sup>15</sup> Ab initio calculations are employed to gauge the relative stabilities of ions and radicals and to assess Franck–Condon effects in vertical neutralization of pyridinium cations.

## EXPERIMENTAL

Measurements were carried out on a tandem quadrupole acceleration–deceleration mass spectrometer, as described previously.<sup>16</sup> Cation-radicals were produced by 70 eV electron impact ionization. Protonation and deuteration were carried out, respectively, with methane (Matheson, 99.9%), water, isobutane (Matheson, 99.9%), anhydrous ammonia (Matheson), methylamine (Matheson), CD<sub>4</sub> (Matheson, 99%D), D<sub>2</sub>O (Cambridge Isotope Laboratories, 99.9% D) and ammonia-d<sub>3</sub> (Matheson, 99% D) in a tight ion source of our design. Pyridine (Fisher, reagent grade) and pyridine-d<sub>5</sub> (Cambridge Isotope Laboratories, 99.5%D) were used as received. The samples were degassed by several freeze–pump–thaw cycles before the measurements. The ionization conditions were electron energy 100 eV, emission current 1 mA and temperature 180–200 °C. The reagent gas pressure in the ion source was adjusted to 0.1–0.2 Torr (1 Torr = 133.3 Pa) to achieve  $[M + H, D]^+ / [M^{++}] > 10$  in most instances. Prior to deuteration experiments, the ion source and the inlet system were treated with D<sub>2</sub>O at 10<sup>−5</sup> Torr for 30–40 min. Stable precursor ions with lifetimes of 30–40 μs were accelerated to 8140–8160 eV kinetic energy and neutralized by collisions with dimethyl disulfide, which was admitted to the collision cell at a pressure to achieve 70% transmittance of the precursor ion beam.



Scheme 1.

Reionization of the fast neutral intermediates was carried out at oxygen pressures such as to achieve 70% transmittance of the ion beam. For standard NRMS,<sup>16</sup> reionization in a fixed collision cell sampled neutrals with lifetimes of 4.3–4.4  $\mu\text{s}$ . In variable-time NRMS,<sup>12,13</sup> the observation times for neutral dissociations were varied in three steps between 0.4 and 2.0  $\mu\text{s}$ ; 40–60 scans were collected per spectrum at a scan rate of  $1 \text{ u s}^{-1}$ , corresponding to 75 data points per peak. The spectra were reproduced on different days over a period of several months.

## CALCULATIONS

Standard ab initio calculations were carried out using the Gaussian 92 and Gaussian 94 suites of programs.<sup>17</sup> Geometries were fully optimized with Hartree–Fock level calculations that employed the 6–31G(d,p) basis set. Spin-unrestricted Hartree–Fock calculations (UHF) were used for all open-shell species. Local potential energy minima were characterized by analytical harmonic frequencies calculated with HF/6–31G(d,p) to give all positive values. The calculated frequencies were scaled by 0.893 and used to obtain zero-point vibrational energies.<sup>18</sup> To account in part for electron correlation, Møller–Plesset perturbation theory,<sup>19</sup> truncated at second order, MP2 (frozen core), was used for single-point calculations with the larger 6–311G(2d,p) basis set using the HF/6–31G(d,p) optimized geometries. UHF calculations of radicals showed  $\langle S^2 \rangle$  values around 1.1, indicating spin contamination by low-lying quartet states. This was corrected in part by annihilating the higher spin states<sup>20</sup> by Schlegel’s spin projection method.<sup>21</sup> The energetics of radical dissociations were also addressed by density-functional theory calculations<sup>22</sup> that were recently shown to give good results for a variety of radicals while avoiding spin contamination problems.<sup>23,24</sup> A hybrid method was applied that used Becke’s three-parameter functional (B3LYP)<sup>25</sup> in the form  $A E_x^{\text{Slater}} + (1 - A) E_x^{\text{UHF}} + B E_c^{\text{VWN}} + C E_c^{\text{non-local}}$ , where  $E_c^{\text{VWN}}$  is Vosko *et al.*’s local correction functional<sup>26</sup> and  $E_c^{\text{non-local}}$  is given by the expression of Lee *et al.*<sup>27</sup> These B3LYP/6–311G(2d,p) single-point calculations used the UHF/6–31G(d,p) optimized geometries, frequencies and 298 K enthalpy corrections.

## RESULTS

Pyridine is the presumed product of N–H,D bond cleavage in pyridinium radicals (Scheme 1). NR mass spectra of  $1^{+\cdot}$  and [pyridine- $d_5$ ] $^{+\cdot}$  ( $5^{+\cdot}$ ) were therefore obtained for reference (Fig. 1). Both  $1^{+\cdot}$  and  $5^{+\cdot}$  gave substantial survivor ions, consistent with the stability of pyridine molecules and cation-radicals. The NR spectra are similar to the standard 70 eV electron impact spectra of **1** and **5** and show ions due to loss of H or D ( $m/z$  78 and 82, respectively), products of HCN or DCN elimination ( $m/z$  52 and 56, respectively) and their dehy-

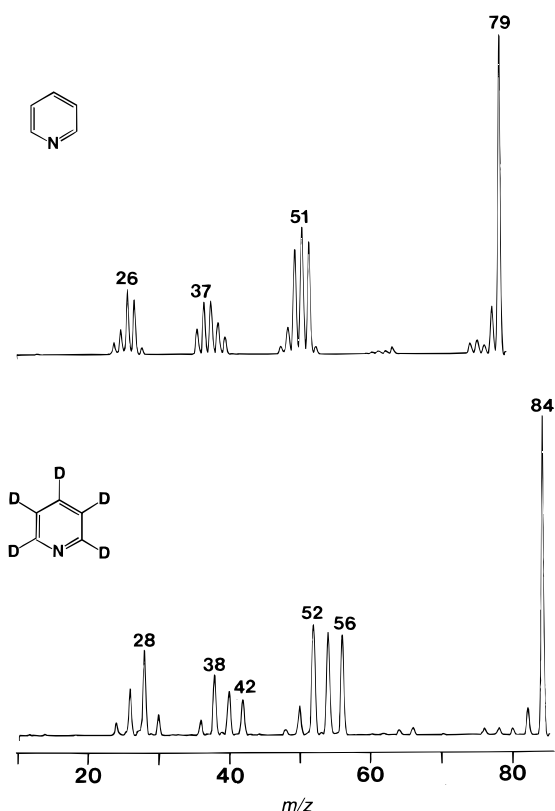


**Figure 1.** Neutralization–reionization [ $\text{CH}_3\text{SSCH}_3$  (70%T)/ $\text{O}_2$  (70%T)] mass spectra of (top) pyridine $^{+\cdot}$  ( $1^{+\cdot}$ ) and (bottom) pyridine- $d_5^{+\cdot}$  ( $5^{+\cdot}$ ).

drogenation products,  $\text{C}_3\text{H}_{0-2}^+$  and  $\text{C}_2\text{H}_{0-2}\text{N}^+$  ring fragments and  $\text{HCN}^{+\cdot}$  or  $\text{DCN}^{+\cdot}$  (Fig. 1). Interestingly, the NR spectrum obtained by slightly exothermic neutralization with dimethyl disulfide, for which  $\Delta\text{IE} = \text{IE}_v(1) - \text{IE}_v(\text{CH}_3\text{SSCH}_3) = 0.64 \text{ eV}$ ,<sup>28</sup> showed less dissociation than did the spectrum obtained with endothermic neutralization with cyclopropane,  $\Delta\text{IE} = -0.6 \text{ eV}$ ,<sup>11</sup> however, the trends in ring fragmentations were similar for both neutralization targets. Compared with electron impact ionization, the NR spectra showed slightly enhanced relative abundances of  $\text{C}_4\text{H}_2^{+\cdot}$ ,  $\text{C}_3\text{HN}^{+\cdot}$  and  $\text{HCN}^{+\cdot}$  as distinguished by deuterium labeling. These corresponded to reionization of stable molecules and may indicate dissociations of neutral pyridine caused by vertical electron transfer. Pyridine has a dense manifold of  $\pi \rightarrow \pi$ ,  $n \rightarrow \pi$  and Rydberg excited states<sup>29,30</sup> that can be accessed by photon absorption or low-energy electron excitation.<sup>29,30</sup> In vertical neutralization, electron capture in a vacant orbital, followed by internal conversion of the excited state to the ground  $^1\text{A}_1$  state, may provide a mechanism for excitation of pyridine molecules and cause their unimolecular dissociations, as discussed recently for aromatic amines.<sup>31</sup>

Neutralization–reionization of protonated pyridine, here denoted as  $1\text{H}^+$  regardless of its structure, also gave substantial survivor ions attesting to the stability of the intermediate pyridinium radicals (Fig. 2). The NR fragmentations of  $1\text{H}^+$  comprised loss of  $\text{H}^{\cdot}$  ( $m/z$  79) and  $\text{HCN}$  ( $m/z$  53) and formation of  $\text{HCNH}^+$  ( $m/z$  28), in addition to the dissociations also observed in the NR

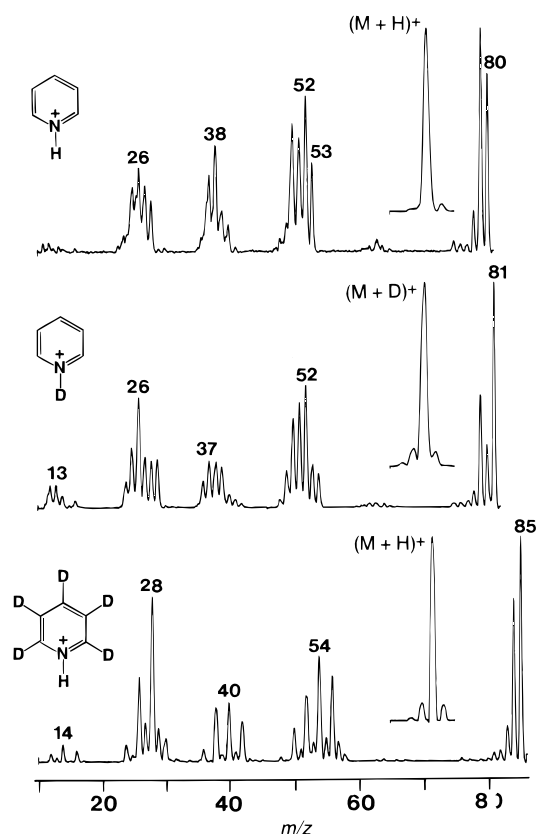


**Figure 2.** Neutralization-reionization ( $CH_3SSCH_3$  (70%T)/ $O_2$  (70%T)) mass spectra. Top,  $1H^+$  from protonation with  $NH_4^+$ ; middle,  $1D^+$  from deuteration with  $ND_4^+$ ; bottom,  $5H^+$  from protonation with  $NH_4^+$ . Insets show the  $[M+H]^+$  or  $[M+D]^+$  regions in the chemical ionization spectra.

spectrum of  $1^{++}$  (Fig. 1). Deuterium labeling showed H-D exchange prior to ring cleavages. For example,  $1D^+$  and  $5H^+$  eliminated HCN and DCN in 1:1 and 1:3 ratios, respectively (Fig. 2). The  $[m/z\ 78]/[m/z\ 79]$  ratio from NR of  $1H^+$  (0.18) was slightly higher than that in the NR spectrum of  $1^{++}$  (0.15, see above). This was due to the combined contributions of H loss from high-energy  $1^{++}$  formed by NR and elimination of  $H_2$  from reionized  $1H^+$ . However, these effects were rather small.

The NR spectra clearly depended on the gas-phase acid used to protonate **1** (Fig. 3). The relative abundances of survivor ions markedly decreased with the increasing protonation exothermicity, expressed as the difference in proton affinities,  $\Delta PA$ .<sup>2</sup> In the series methylamine ( $\Delta PA = 23\ kJ\ mol^{-1}$ ), ammonia ( $\Delta PA = 70\ kJ\ mol^{-1}$ ), isobutane ( $\Delta PA = 122\ kJ\ mol^{-1}$ ) and methane ( $\Delta PA = 380\ kJ\ mol^{-1}$ ), the respective abundances of reionized  $[MH^+]$ , relative to the sum of integrated NR ion abundances ( $\Sigma_{NR}$ ), were 7.8, 7.6, 3.7 and 0.9%. Hence, the precursor ion internal energy affected the stability of the intermediate radical and/or the reionized cation. Note, however, that ions  $1H^+$  are very stable and their dissociations should not be susceptible to small internal energy variations. The dissociation by loss of H to give  $1^{++}$  requires  $505\ kJ\ mol^{-1}$  (from the ion heats of formation<sup>2,28</sup>) and could thus occur only in a fraction of highly excited ions. The above-mentioned protonation exothermicities alone

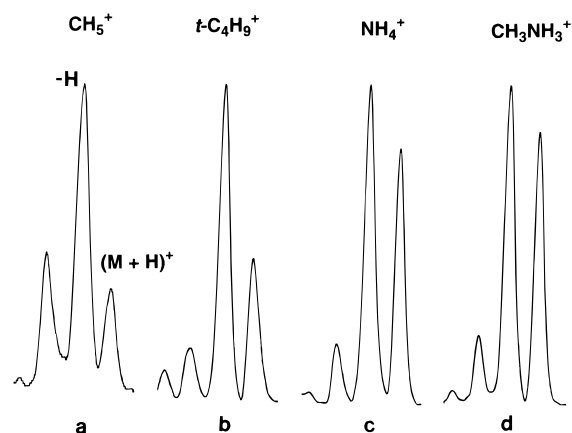


**Figure 3.** Survivor ion regions in the NR spectra of  $1H^+$  from protonation with (a)  $CH_5^+$ , (b)  $t-C_4H_9^+$ , (c)  $NH_4^+$  and (d)  $CH_3NH_3^+$ . Collision conditions as in Fig. 2.

were insufficient to promote ion unimolecular dissociations.

Deuteration of **1**, followed by NR of  $1D^+$ , gave the spectra shown in Figs 2 (middle) and 4. Clearly, loss of both H and D occurred on neutralization-reionization and the relative abundances of  $[1D-H]^+$  and  $[1D-D]^+$  depended on the precursor ion internal energy, as limited by the deuteration exothermicity. The more exothermic deuteration with  $D_3O^+$  caused more dissociation on NR of  $1D^+$  than did deuteration with  $ND_4^+$  (Fig. 4). However, the  $[1D-H]^+/[1D]^+$  ratio expressing the loss of the original C-bound hydrogen atoms decreased upon increasing the precursor ion internal energy, e.g. 0.30 and 0.26 for deuteration with  $ND_4^+$  and  $D_3O^+$ , respectively. In contrast, the extent of D loss, expressed by the  $[1D-D]^+/[1D]^+$  ratio, was greater, both absolutely and relatively, following deuteration with  $D_3O^+$  (1.7) than with  $ND_4^+$  (0.8). Hence the specificity for the loss of the deuterium introduced by the gas-phase acid was greater for the more exothermic deuteration with  $D_3O^+$  than with the milder  $ND_4^+$ .

Exothermic protonations of **5**, followed by NR, gave results similar to those from deuteration of **1** (Fig. 5). The loss of D from  $5H^+$  was comparable for the ions

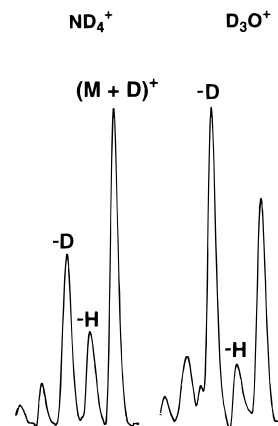


**Figure 4.** Survivor ion regions in the NR spectra of  $1D^+$  from protonation with  $ND_4^+$  and  $D_3O^+$ . Collision conditions as in Fig. 2.

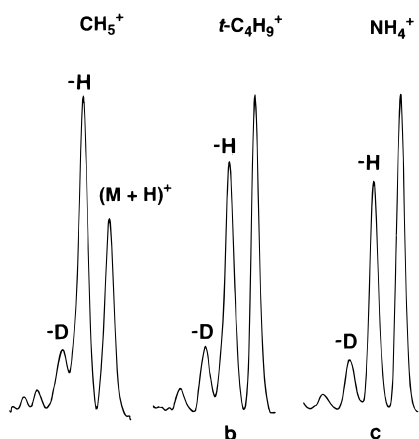


**Figure 5.** Survivor ion regions in the NR spectra of  $5\text{H}^+$  from protonation with (a)  $\text{CH}_5^+$ , (b)  $t\text{-C}_4\text{H}_9^+$  and (c)  $\text{NH}_4^+$ . Collision conditions as in Fig. 2.

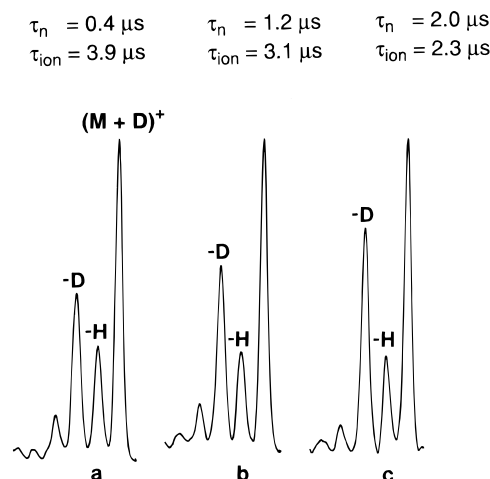


**Figure 6.** Survivor ion regions in the variable-time NR spectra of  $1\text{D}^+$  for neutral observation times ( $\tau_n$ ): (a) 0.4, (b) 1.2 and (c) 2.0  $\mu\text{s}$ .

generated by protonation with  $\text{NH}_4^+$  and  $t\text{-C}_4\text{H}_9^+$ , as shown by the  $[\text{5H} - \text{D}]^+ / [\text{5H}]^+$  ratios, which were 0.18 and 0.17, respectively. The highly exothermic protonation with  $\text{CH}_5^+$  gave a ratio of 0.3. However, NR of the high-energy  $5\text{H}^+$  from protonation with  $\text{CH}_5^+$  gave the greatest  $[\text{5H} - \text{H}]^+ / [\text{5H} - \text{D}]^+$  ratio (5.5) compared with those for the less excited  $5\text{H}^+$  from protonations with  $t\text{-C}_4\text{H}_9^+$  and  $\text{NH}_4^+$ , which were 4.1 and 4.3, respectively. Hence, the loss of the C-bound deuterium was least important in the highest energy radicals or ions.

To assess the contributions of neutral and ion dissociations in NR, we obtained variable-time NR spectra of  $\text{ND}_4^+$ -deuterated pyridine ( $1\text{D}^+$ ) at 0.4, 1.2 and 2.0  $\mu\text{s}$  observation times for the neutrals and the respective 3.9, 3.1 and 2.3  $\mu\text{s}$  observation times for the ions after reionization (Fig. 6). The spectra showed that the  $[\text{1D} - \text{D}]^+ / [\text{1D} - \text{H}]^+$  ratios, which gauged the specificity of the N-deuteron loss, increased with the increasing observation time for radical  $1\text{D}^+$  and the

decreasing observation time for reionized  $1\text{D}^+$ . Hence, increasing the reaction time for neutral dissociations increased the specificity for the loss of the N-bound deuterium from  $1\text{D}^+$ , as discussed later.

The energetics of the ionic and radical isomers was addressed by MP2/6-311(2d,p) ab initio calculations for  $1\text{H}^+ - 4\text{H}^+$  and by UMP2 and B3LYP/6-311G(2d,p) calculations for  $1\text{H}^- - 3\text{H}^-$  (Table 1). We<sup>8</sup> and others<sup>4</sup> have shown previously that this intermediate level of theory provided excellent proton affinities of nitrogen bases and thus represented a good compromise of accuracy and economy.<sup>8</sup> The HF/6-31G(d,p) optimized structures of **1** and  $1\text{H}^+ - 4\text{H}^+$  are given in Fig. 7. The optimized structure of **1** was similar to those from previous ab initio calculations<sup>11,32</sup> and showed a reasonable agreement with experimental data.<sup>33</sup> The calculated proton affinities for N, C-2, C-3 and C-4 (Table 2) agreed closely with those reported by Hillbrand *et al.*<sup>4</sup> and showed that the nitrogen atom must

**Table 1.** *Ab initio* energies of **1**,  $1\text{H}^+ - 4\text{H}^+$  and  $1\text{H}^- - 3\text{H}^-$

Species	HF/6-31G(d,p) <sup>a</sup>	MP2/6-311G(2d,p) <sup>a,b</sup>	$\langle S^2 \rangle$	ZPVE <sup>c</sup>	$H_{298} - H_0$ <sup>c</sup>
<b>1</b>	-246.704 612	-247.647 935	0	223	13.9
$1\text{H}^+$	-247.083 907	-248.013 331	0	258	14.3
$2\text{H}^-$	-246.988 631	-247.908 364	0	247	15.7
$3\text{H}^+$	-247.006 471	-247.919 064	0	247	16.1
$4\text{H}^+$	-246.971 800	-247.899 503	0	244	16.1
$1\text{H}^-$	-247.252 595	-248.163 798	1.1	242	16.5
		-248.186 744 <sup>b</sup>	0.81 <sup>b</sup>		
$1\text{H}^-$ (VN) <sup>d</sup>		-248.158 508	1.1		
		-248.178 665 <sup>b</sup>	0.83 <sup>b</sup>		
$2\text{H}^-$	-247.253 681	-248.147 217	1.2	241	16.3
		-248.176 599 <sup>b</sup>	0.88 <sup>b</sup>		
$3\text{H}^-$	-247.254 414	-248.149 165	1.2	239	16.3
		-248.178 348 <sup>b</sup>	0.88 <sup>b</sup>		
$3\text{H}^-$ (VN) <sup>d</sup>		-248.149 091	1.1		
		-248.175 737 <sup>b</sup>	0.85 <sup>b</sup>		

<sup>a</sup> In units of hartree; 1 hartree = 2625.5 kJ mol<sup>-1</sup>.

<sup>b</sup> After annihilation of higher spin states.

<sup>c</sup> Zero-point vibrational energies corrected by 0.893 and 298 K enthalpy corrections in kJ mol<sup>-1</sup>.

<sup>d</sup> Single-point calculations on optimized ion geometries.

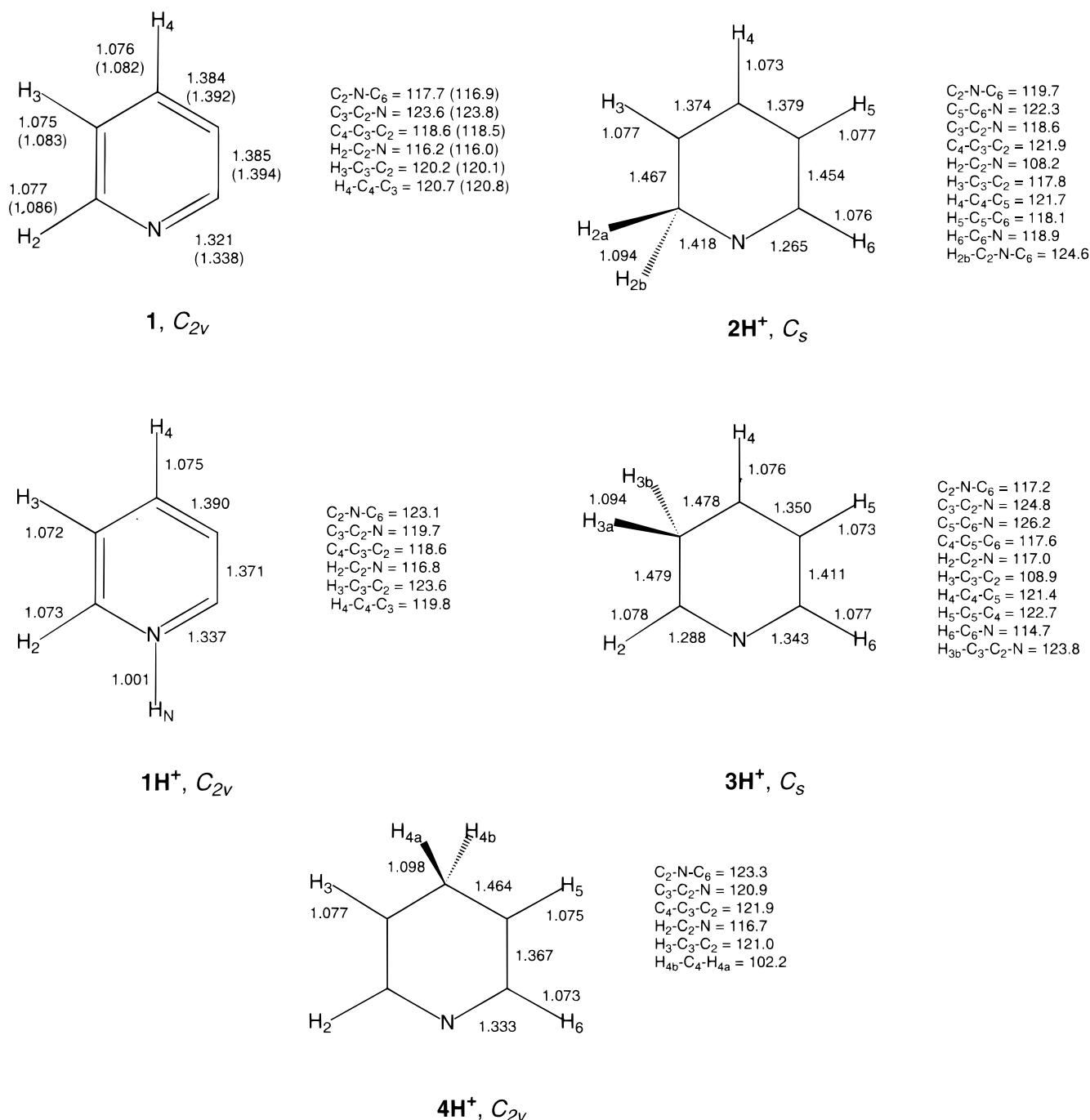


**Figure 7.** RHF/6-31G(d,p) optimized structures of **1** and **1H<sup>+</sup>**, **2H<sup>+</sup>**, **3H<sup>+</sup>** and **4H<sup>+</sup>**. Bond lengths in ångstroms, bond and dihedral angles in degrees. Values in parentheses are experimental data from the microwave spectra of **1**.

be the preferred protonation site in **1**. The proton affinity of **1** was in excellent agreement with the tabulated value (924 kJ mol<sup>-1</sup>).<sup>2</sup> The data also showed that pyridine should be protonated exclusively at N with gas-phase acids of PA ≥ 690 kJ mol<sup>-1</sup> to give the single pyridinium isomer **1H<sup>+</sup>**. Protonation with H<sub>3</sub>O<sup>+</sup> [PA(H<sub>2</sub>O) = 690 kJ mol<sup>-1</sup>] could yield a small fraction of **3H<sup>+</sup>**, but not **2H<sup>+</sup>** or **4H<sup>+</sup>**. Protonation with CH<sub>5</sub><sup>+</sup> was exothermic for all positions in **1** and could produce mixtures of isomers.

Electron attachment to pyridinium ions yields the corresponding radicals that were investigated by UMP2 and B3LYP calculations for **1H<sup>•</sup>**, **2H<sup>•</sup>** and **3H<sup>•</sup>** (Fig. 8,

Table 1). Isomer **4H<sup>•</sup>** corresponding to the least stable cation **4H<sup>+</sup>** was not studied. In contrast to the cations, radicals **1H<sup>•</sup>**, **2H<sup>•</sup>** and **3H<sup>•</sup>** showed much smaller differences in their relative stabilities (Table 2). Both the UMP2 and B3LYP calculations showed that the pyridinium radicals were bound against dissociations to pyridine and hydrogen atom. The B3LYP reaction endothermicities were about 40 kJ mol<sup>-1</sup> greater than those from UMP2, indicating higher stabilities for the pyridinium radicals. This probably reflects incomplete corrections of spin contamination in the radicals by the spin projection method used.<sup>21</sup> A higher level treatment of electron correlation would probably result in further

**Table 2. Relative enthalpies from MP2 and B3LYP/6-311G(2d,p) calculations**

Reaction	Proton affinity <sup>a</sup>	$\Delta H_{f,0}$		$\Delta H_{f,298}$	
		MP2	B3LYP <sup>b</sup>	MP2	B3LYP
<b>1</b> → <b>1H</b> <sup>+</sup>	924				
<b>1</b> → <b>2H</b> <sup>+</sup>	658				
<b>1</b> → <b>3H</b> <sup>+</sup>	686				
<b>1</b> → <b>4H</b> <sup>+</sup>	637				
<b>1H</b> <sup>•</sup> → <b>1</b> + H <sup>•</sup>		83	126	87	130
<b>1H</b> <sup>•</sup> (VN) <sup>c</sup> → <b>1</b> + H <sup>•</sup>		62	106	66	110
<b>2H</b> <sup>•</sup> → <b>1</b> + H <sup>•</sup>		58	98	62	102
<b>3H</b> <sup>•</sup> → <b>1</b> + H <sup>•</sup>		64	100	68	104
<b>3H</b> <sup>•</sup> (VN) <sup>c</sup> → <b>1</b> + H <sup>•</sup>		57		61	

<sup>a</sup> At 298 K in kJ mol<sup>-1</sup>.

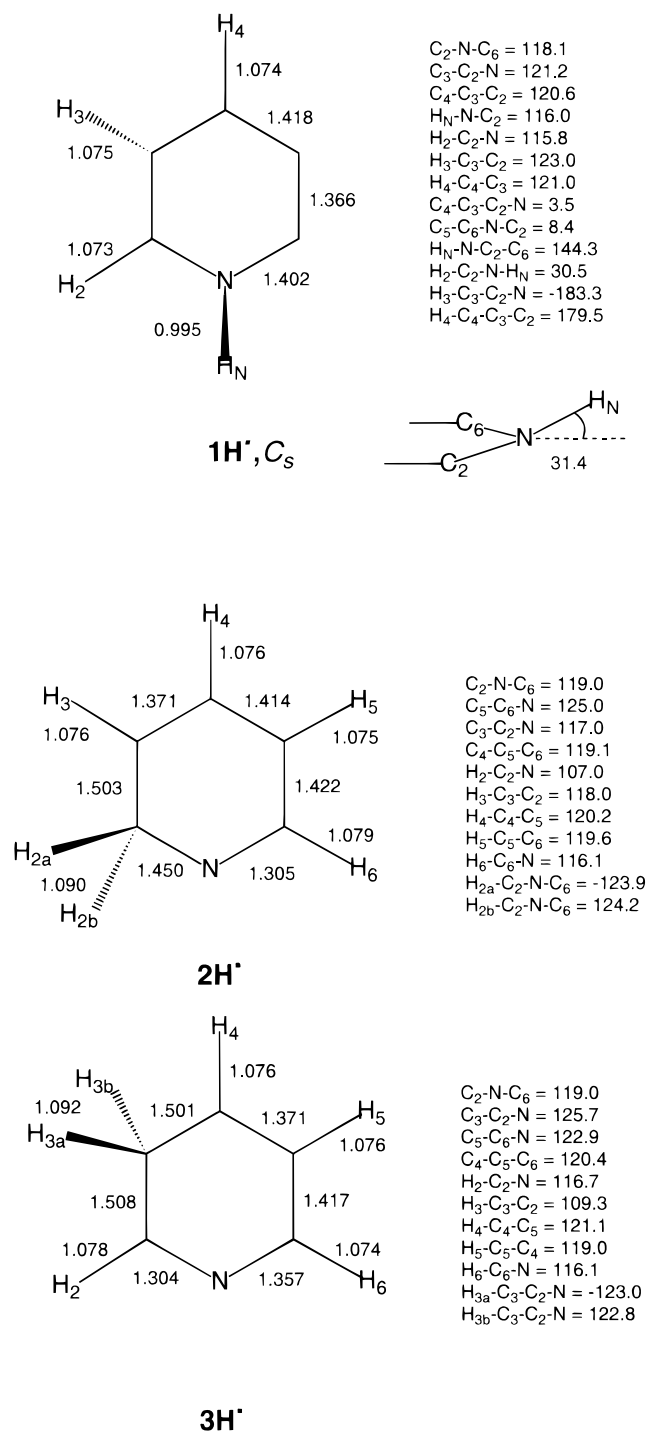
<sup>b</sup> The B3LYP/6-311G(2d,p) total energies were -248.352754, -248.910272, -0.502156, -248.902469, -248.898856 and -248.899337 hartree for **1**, **1H**<sup>•</sup>, H<sup>•</sup>, **1H**<sup>•</sup>(VN), **2H**<sup>•</sup> and **3H**<sup>•</sup>, respectively.

<sup>c</sup> Vertically neutralized radicals.

stabilization of the pyridinium radicals. **1H**<sup>•</sup> was the most stable isomer, which was bound by 87–130 kJ mol<sup>-1</sup> against dissociation to **1** and hydrogen atom. Vertical neutralization of **1H**<sup>+</sup> was calculated to be accompanied by moderate Franck–Condon effects, estimated at 20–21 kJ mol<sup>-1</sup>, that were deposited in **1H**<sup>•</sup> (Table 2). Hence, **1H**<sup>•</sup> formed by vertical reduction of a vibrationally relaxed (all  $\nu = 0$ ) **1H**<sup>+</sup> should be thermodynamically and kinetically stable. The reaction path for the NH bond dissociation was not studied in detail for the pyridinium radicals. Clearly, the possible presence of an activation barrier would provide further kinetic stabilization for the radical as found previously for imidazole radicals.<sup>8</sup>

The Franck–Condon effects in neutralization of **1H**<sup>+</sup> are due to differences in the cation and radical geometries (Figs 7 and 8). The equilibrium structure of **1H**<sup>•</sup> shows C-2–N and C-3–C-4 bonds which are longer than those in **1H**<sup>+</sup>. The nitrogen atom in **1H**<sup>•</sup> is pyramidal, while the H<sub>N</sub>–N bond is deflected 31.4° out of the C-2–N–C-6 plane. These geometry differences between **1H**<sup>+</sup> and **1H**<sup>•</sup> indicate that the vibrational excitation on vertical neutralization will be initially stored in the ring-breathing and H–N out-of-plane deformation vibrations. These modes are relatively soft in **1H**<sup>•</sup>, e.g. 592 and 973 cm<sup>-1</sup> for the ring breathing (a') and 380, 732 and 836 cm<sup>-1</sup> for the N–H and C–H out-of-plane (a'') deformation modes and should be readily excited in the ion. This means that Franck–Condon effects will be diminished in vertical neutralization of vibrationally excited **1H**<sup>+</sup>. Vibrational excitation in precursor ions has been shown previously to broaden the distribution of internal energies in neutrals formed by collisional electron transfer.<sup>34</sup>

Radicals **2H**<sup>•</sup> and **3H**<sup>•</sup> were also calculated to be bound against hydrogen loss (Table 2). Franck–Condon effects in vertical reduction of **3H**<sup>+</sup> amounted to only 7 kJ mol<sup>-1</sup>, attesting to the good match of the cation and radical equilibrium geometries (Figs 7 and 8). The small difference in the radical stabilities caused large differences in the ion vertical recombination energies (RE<sub>v</sub>)


**Figure 8.** UHF/6-31G(d,p) optimized structures of **1H**<sup>•</sup>, **2H**<sup>•</sup> and **3H**<sup>•</sup>.

and radical adiabatic ionization energies (IE<sub>a</sub>). The MP2 data in Table 1 allow one to estimate IE<sub>a</sub> for **1H**<sup>•</sup> and **3H**<sup>•</sup> as 4.71 and 7.04 eV, respectively, whereas the corresponding RE<sub>v</sub> values for **1H**<sup>+</sup> and **3H**<sup>+</sup> are 4.48 and 6.97 eV, respectively. Vertical electron transfer from dimethyl disulfide (IE<sub>v</sub> = 8.96 eV)<sup>28</sup> is thus 4.47 and 1.99 eV endothermic for **1H**<sup>+</sup> and **3H**<sup>+</sup>, respectively. Since the neutralization cross-sections generally decrease with increasing differences between the RE<sub>v</sub>(ion) and IE<sub>v</sub>(target),<sup>7,15</sup> collisional neutralization with dimethyl disulfide could be more efficient for **3H**<sup>+</sup> than for the more stable **1H**<sup>+</sup>.

---

## DISCUSSION

---

The behavior of pyridinium ions and radicals on neutralization and reionization is now discussed in the light of the energy data provided by ab initio calculations. The energy data showed clearly that, under thermal conditions, protonation of pyridine with  $\text{CH}_3\text{NH}_3^+$ ,  $\text{NH}_4^+$  and  $t\text{-C}_4\text{H}_9^+$  must have occurred at the nitrogen atom. This requirement is not mitigated by the thermal energy in **1** undergoing protonation at 473 K. Analysis of the vibrational energy distribution in thermal **1**, according to Dunbar,<sup>35</sup> showed a negligible ( $<10^{-3}$ ) fraction of molecules with  $E_{\text{vib}} > 40 \text{ kJ mol}^{-1}$  at 473 K. The species sampled for collisional neutralization was therefore pure pyridinium  $1\text{H}^+$  or its isotopomers, because the other ion isomers were energetically inaccessible. Protonation with  $\text{H}_3\text{O}^+$  and  $\text{CH}_5^+$  could form  $3\text{H}^+$  or the other ion isomers. However, bimolecular reactions, e.g.  $3\text{H}^+ + 1 \rightarrow 1\text{H}^+ + 1$ , are substantially exothermic and can be expected to deplete the population of the C-protonated isomers in the ion source. Such reactions are difficult to avoid in a standard chemical ionization ion source even at a large excess of the reagent gas. Protonations with different gas-phase acids evidently produced ions of different internal energies. The ion internal energy was passed on to the radical and modified by the Franck–Condon effects in vertical neutralization.<sup>34</sup> The experiments showed that, in the absence of large Franck–Condon factors predicted by theory, the stability of the neutralized  $1\text{H}^\cdot$  was mainly determined by the internal energy of the precursor ion.

In contrast, the selectivity for loss of N-bound H or D showed two trends. First, increasing the internal energy of  $5\text{H}^+$  and  $1\text{D}^+$  resulted in an increased specificity for the loss of the N-bound proton or deuteron, while at the same time depleting the fraction of surviving ions. This effect can be unequivocally attributed to specific loss of N-bound H or D in the radicals ( $1\text{H}^\cdot$ ,  $1\text{D}^\cdot$  and  $5\text{H}^\cdot$ ), which are much less stable than their corresponding ions. It also suggested that unimolecular isomerizations of  $1\text{H}^\cdot$  to  $2\text{H}^\cdot$ – $4\text{H}^\cdot$  did not compete with the hydrogen loss at higher internal energies. The slightly increased total but not relative loss of D from  $5\text{H}^+$  by  $\text{CH}_5^+$  protonation may be due to a minor fraction of C-protonated isomers; however, this evidence is not fully conclusive, because of the large effect on the dissociations of the ion internal energy. The results also showed that specific losses of C-bound H or D from  $1\text{H}^\cdot$  or  $5\text{H}^\cdot$  did not occur to produce pyridine ylides.<sup>11</sup> These have been calculated<sup>11</sup> to be  $\sim 200 \text{ kJ mol}^{-1}$  less stable than **1** and their formation thus would be expected to become competitive at higher energies only.

Second, at low radical excitation, resulting from less exothermic protonation with  $\text{NH}_4^+$  or  $\text{ND}_4^+$ , a substantial fraction of  $1\text{H}^\cdot$  and  $1\text{D}^\cdot$  survived to be reionized. The variable-time NR measurements showed that increasing the observation time for neutral dissociations increased the contribution of the specific loss of the N-bound D. This strongly indicated that even at low excitation, the dissociating radicals preferred to lose the nitrogen-bound deuterium. One may conclude that the latter dissociation is also kinetically preferred over

hydrogen rearrangements in low-energy dissociating radicals.

The inverse correlation between the specificity for H or D loss on the one hand and the fraction of survivor ions and the observation time for their dissociations on the other strongly indicates that the non-specific loss was due to ion dissociations. Collisional reionization is always accompanied by energy deposition, which results in a broadened internal energy distribution in the ions formed.<sup>34,36</sup> Although the internal energy distribution in reionized  $1\text{H}^+$  was not determined, deposition of up to several electronvolts was possible by analogy with other systems.<sup>34,36</sup> The energy barriers to isomerizations that would scramble the N- and C-bound hydrogens, e.g.  $1\text{H}^+ 2\text{H}^+$ , were unknown, but could be estimated at 250–300  $\text{kJ mol}^{-1}$  based on calculations for other heterocyclic systems.<sup>8,11</sup> Hence, the high endothermicity for hydrogen loss (505  $\text{kJ mol}^{-1}$ ) should make such hydrogen migrations energetically possible and kinetically competitive in high-energy dissociating pyridinium cations.<sup>8</sup> In an alternative mechanism, pyridine ylide ions have been calculated<sup>11</sup> to be only 20–30  $\text{kJ mol}^{-1}$  less stable than  $1^{++}$  and could be accessible by loss of C-bound H from  $1\text{H}^+$ . Unfortunately, the  $m/z$  28 signature fragment ion for the pyridine-2-ylide ion<sup>11</sup> was completely obliterated in the NR spectra of  $1\text{H}^+$ , leaving the question of ylide ion formation open. From a different point of view, the presence of highly endothermic ion dissociations revealed by the variable-time measurements confirmed that there must be a substantial fraction of ions that acquired  $>5 \text{ eV}$  internal energy on collisional reionization.

---

## CONCLUSIONS

---

The results of ab initio calculations and variable-time neutralization–reionization measurements showed that gas-phase protonation of pyridine under thermal conditions formed exclusively the most stable N-protonated cation. The highly exothermic protonation with  $\text{CH}_5^+$  may form a small fraction of C-protonated isomers that were difficult to characterize. Neutralization–reionization spectra showed superposition of radical and ion dissociations that were deconvoluted to provide unequivocal structure information. Theory and experiment were in accord in showing that the  $1\text{H}$ -pyridinium radical was a stable species when formed by vertical neutralization of N-protonated pyridine.

## Acknowledgements

Financial support of this work by the National Science Foundation (Grant CHE-9412774) is gratefully acknowledged. The ab initio computations were conducted by using the resources of the Cornell Theory Center, which receives major funding from the National Science Foundation and New York State with additional support from the Advanced Research Projects Agency, the National Center for Research Resources at the National Institutes of Health, IBM Corporation and members of the Corporate Research Institute. We also thank Dr Graham A. McGibbon for a preprint of Ref. 11.

## REFERENCES

1. M. T. Bowers (Ed.) *Gas-Phase Ion Chemistry*, Vol. 2, pp. 1–51. Academic Press, New York (1979).
2. S. G. Lias, J. F. Liebman and R. D. Levin, *J. Phys. Chem. Ref. Data* **13**, 695 (1984).
3. E. F. V. Scriven, in *Comprehensive Heterocyclic Chemistry*, edited by A. R. Katritzky, C. W. Rees, A. J. Boulton and A. McKillop, Vol. 2, p. 170. Pergamon Press, Oxford (1984).
4. C. Hillebrand, M. Klessinger, M. Eckert-Maksic and Z. B. Maksic, *J. Phys. Chem.* **100**, 9698 (1996).
5. J. E. Szulejko and T. B. McMahon, *J. Am. Chem. Soc.* **115**, 7839 (1993).
6. A. W. McMahon, F. Chadikun and A. G. Harrison, *Int. J. Mass Spectrom. Ion Processes* **87**, 275 (1989).
7. J. L. Holmes, *Mass Spectrom. Rev.* **8**, 513 (1989).
8. V. Q. Nguyen and F. Tureček, *J. Mass Spectrom.* **31**, 1173 (1996).
9. M. J. Nold and C. Wesdemiotis, *J. Mol. Spectrosc.* **31**, 1169 (1996).
10. S. Beranova, J. Cai and C. Wesdemiotis, *J. Am. Chem. Soc.* **117**, 9492 (1995).
11. D. Lavorato, J. K. Terlouw, T. K. Dargel, W. Koch, G. A. McGibbon and H. Schwarz, unpublished data.
12. D. W. Kuhns, T. B. Tran, S. A. Shaffer and F. Tureček, *J. Phys. Chem.* **98**, 4845 (1994).
13. D. W. Kuhns and F. Tureček, *Org. Mass Spectrom.* **29**, 463 (1994).
14. M. Sadilek and F. Tureček, *J. Phys. Chem.* **100**, 15027 (1996).
15. M. Sadilek and F. Tureček, *J. Phys. Chem.* **100**, 224 (1996).
16. F. Tureček, M. Gu and S. A. Shaffer, *J. Am. Soc. Mass Spectrom.* **3**, 493 (1992).
17. M. J. Frisch, G. W. Trucks, M. Head-Gordon, P. M. W. Gill, M. W. Wong, J. B. Foresman, B. G. Johnson, H. B. Schlegel, M. A. Robb, E. S. Replogle, R. Gomperts, J. L. Andres, K. Raghavachari, J. S. Binkley, C. Gonzalez, R. L. Martin, D. J. Fox, D. J. DeFrees, J. Baker, J. J. P. Stewart and J. A. Pople, Gaussian 92, Revision C. Gaussian, Pittsburgh, PA (1992).
18. W. J. Hehre, L. Radom, P. v. R. Schleyer and J. A. Pople, *Ab Initio Molecular Orbital Theory*. Wiley, New York (1986).
19. C. Møller and M. S. Plesset, *Phys. Rev.* **46**, 618 (1934).
20. I. Mayer, *Adv. Quant. Chem.* **12**, 189 (1980).
21. H. B. Schlegel, *J. Chem. Phys.* **84**, 4530 (1986).
22. R. G. Parr and W. Yang, *Density-Functional Theory of Atoms and Molecules*. Oxford University Press, New York (1989).
23. B. S. Jursic, *Chem. Phys. Lett.* **256**, 603 (1996).
24. G. M. Jensen, D. B. Goodin and S. W. Bunte, *J. Phys. Chem.* **100**, 954 (1996).
25. A. D. Becke, *J. Chem. Phys.* **98**, 5648 (1993).
26. S. H. Vosko, L. Wilk and M. Nusair, *Can. J. Phys.* **58**, 120 (1980).
27. C. Lee, W. Yang and R. G. Parr, *Phys. Rev. B* **37**, 785 (1988).
28. S. G. Lias, J. F. Liebman, R. D. Levin and S. A. Kafafi, *NIST Standard Reference Database 19A*. National Institute of Standards and Technology, Gaithersburg, MD (1993).
29. I. C. Walker, M. H. Palmer and A. Hopkirk, *Chem. Phys.* **141**, 365 (1990).
30. K. K. Innes, I. G. Ross and W. R. Moomaw, *J. Mol. Spectrosc.* **132**, 492 (1988).
31. S. A. Shaffer, M. Sadilek and F. Tureček, *J. Org. Chem.* **61**, 5234 (1996).
32. J. B. Foresman, M. Head-Gordon, J. A. Pople and M. J. Frisch, *J. Phys. Chem.* **96**, 135 (1992).
33. F. Mata, M. J. Quintana and G. O. Sørensen, *J. Mol. Struct.* **42**, 1 (1977).
34. V. Q. Nguyen and F. Tureček, *J. Mass Spectrom.* **31**, 843 (1996).
35. R. C. Dunbar, *J. Chem. Phys.* **90**, 7369 (1989).
36. S. Beranova and C. Wesdemiotis, *J. Am. Soc. Mass Spectrom.* **5**, 1093 (1994).

## APPENDIX

Corrected harmonic frequencies ( $\text{cm}^{-1}$ )

Pyridine (1): 390, 414, 588, 643, 695, 750, 882, 959, 976, 1002, 1006, 1011, 1035, 1053, 1056, 1171, 1198, 1341, 1431, 1478, 1598, 1607, 2984, 2984, 2995, 3012, 3019.

1H-Pyridinium ( $1\text{H}^+$ ): 380, 392, 592, 616, 647, 732, 835, 877, 973, 1003, 1005, 1009, 1033, 1036, 1044, 1104, 1176, 1188, 1282, 1367, 1471, 1532, 1619, 1623, 3024, 3041, 3043, 3054, 3055, 3405.

2H-Pyridinium ( $2\text{H}^+$ ): 219, 313, 414, 842, 862, 920, 921, 957, 1002, 1037, 1055, 1111, 1132, 1178, 1272, 1305, 1376, 1387, 1432, 1511, 1627, 2802, 2821, 3008, 3010, 3019, 3040.

3H-Pyridinium ( $3\text{H}^+$ ): 183, 287, 386, 548, 603, 648, 787, 841, 936, 940, 965, 999, 1032, 1074, 1129, 1171, 1181, 1295, 1333, 1354, 1370, 1410, 1534, 1609, 2810, 2834, 3001, 3015, 3019, 3043.

4H-Pyridinium ( $4\text{H}^+$ ): 144, 310, 428, 550, 593, 683, 808, 844, 854, 940, 951, 989, 1021, 1031, 1068, 1129, 1163, 1171, 1234, 1321, 1390, 1426, 1479, 1550, 2777, 2794, 3023, 3024, 3045, 3048.

1H-Pyridinium radical ( $1\text{H}^\cdot$ ): 221, 383, 432, 544, 569, 597, 600, 668, 669, 862, 863, 879, 925, 944, 997, 1045, 1135, 1180, 1286, 1325, 1406, 1444, 1477, 1525, 2990, 2995, 3011, 3020, 3025, 3437.

2H-Pyridinium radical ( $2\text{H}^\cdot$ ): 141, 340, 477, 533, 575, 610, 708, 815, 871, 885, 910, 929, 935, 975, 1058, 1099, 1197, 1234, 1310, 1354, 1377, 1415, 1441, 1461, 2807, 2819, 2961, 2978, 2994, 3010.

3H-Pyridinium radical ( $3\text{H}^\cdot$ ): 139, 347, 496, 534, 581, 614, 714, 735, 816, 879, 902, 913, 927, 974, 1087, 1110, 1144, 1220, 1307, 1341, 1388, 1419, 1451, 1455, 2789, 2798, 2962, 2980, 2994, 3009.